

# Single-Molecule Fluorescence Photoswitching of a Diarylethene–Perylenebisimide Dyad: Non-destructive Fluorescence Readout

Tuyoshi Fukaminato,<sup>\*,†,‡</sup> Takao Doi,<sup>§</sup> Nobuyuki Tamaoki,<sup>†</sup> Katsuki Okuno,<sup>¶</sup> Yukihide Ishibashi,<sup>¶</sup> Hiroshi Miyasaka,<sup>¶</sup> and Masahiro Irie<sup>\*,||</sup>

<sup>†</sup>Research Institute for Electronic Science, Hokkaido University, N20, W10, Kita-ku, Sapporo 001-0020, Japan

<sup>‡</sup>PREST, Japan Science and Technology Agency (JST)

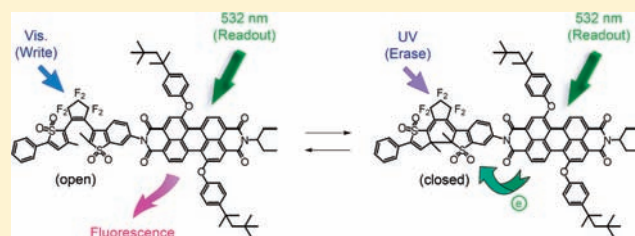
<sup>§</sup>Department of Chemistry and Biochemistry, Graduate School of Engineering, Kyushu University, Motooka 744, Nishi-ku, Fukuoka 819-0395, Japan

<sup>¶</sup>Division of Frontier Materials Science, Graduate School of Engineering Science, and Center for Quantum Science and Technology under Extreme Conditions, Osaka University, Toyonaka, Osaka 560-8531, Japan

<sup>||</sup>Department of Chemistry and Research Center for Smart Molecules, Rikkyo University, Nishi-Ikebukuro 3-34-1, Toshima-ku, Tokyo 171-8501, Japan

**S** Supporting Information

**ABSTRACT:** Single-molecule fluorescence photoswitching plays an essential role in ultrahigh-density (Tbits/inch<sup>2</sup>) optical memories and super-high-resolution fluorescence imaging. Although several fluorescent photochromic molecules and fluorescent proteins have been applied, so far, to optical memories and super-high-resolution imaging, their performance is unsatisfactory because of the absence of “non-destructive fluorescence readout capability”. Here we report on a new molecular design principle of a molecule having non-destructive readout capability. The molecule is composed of acceptor photochromic diarylethene and donor fluorescent perylenebisimide units. The fluorescence is reversibly quenched when the diarylethene unit converts between the open- and the closed-ring isomers upon irradiation with visible and UV light. The fluorescence quenching is based on an electron transfer from the donor to the acceptor units. The fluorescence photoswitching and non-destructive readout capability were demonstrated in solution (an ensemble state) and at the single-molecule level. Femtosecond time-resolved transient and fluorescent lifetime measurements confirmed that the fluorescence quenching is attributed to the intramolecular electron transfer.



## INTRODUCTION

Fluorescent photochromic molecules, which have both photochromic and fluorescent properties in a single molecule, have attracted increasing interest because of their potential applications in optical memories and as molecular switches and fluorescent biological markers.<sup>1–18</sup> A typical example of such molecules is a dyad composed of photochromic and fluorescent dye units, which modulates the fluorescence emission by the photochromic reaction. Not only small organic molecules but also photoactivatable fluorescent proteins (PAFPs),<sup>19</sup> such as “Dronpa”,<sup>20</sup> are suggested as fluorescent photochromic chromophores. Fluorescence photoswitching of such molecules and proteins at the single-molecule level has opened possibilities to develop ultra-high-density (Tbits/inch<sup>2</sup>) optical memories<sup>3–5,20–22,27–29</sup> and super-high-resolution fluorescence imaging.<sup>13,14,25,26,30–35</sup> PAFP contribute significantly to the development of high-resolution imaging.<sup>25,26,31–33</sup>

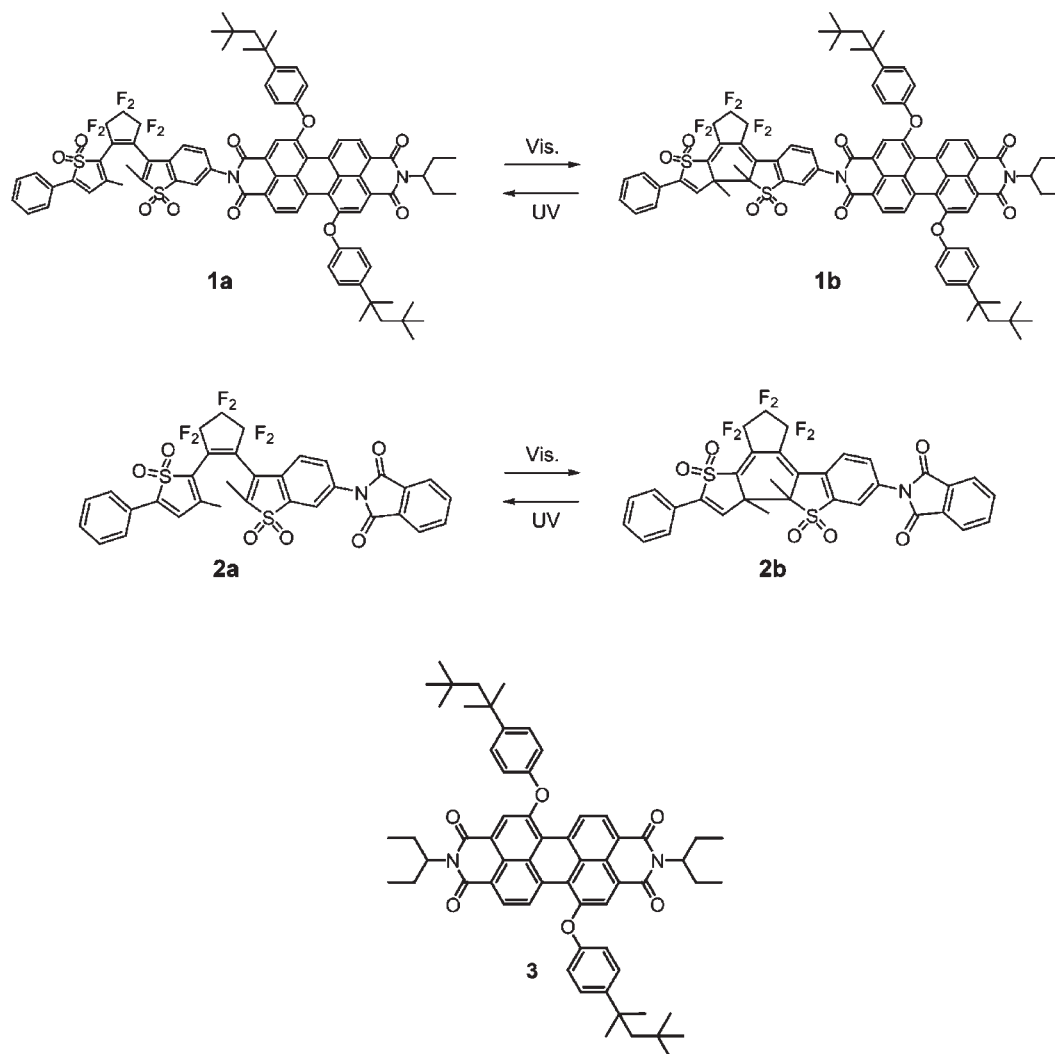
So far, we have developed various types of fluorescent diarylethene (DE) derivatives for single-molecule optical memories.<sup>3–5,9–11</sup> In a series of our studies, two types of fluorescence quenching mechanisms are employed, intramolecular energy transfer<sup>3–5</sup> and electron transfer mechanisms.<sup>9–11</sup> To photoswitch the fluorescence by the former mechanism, we

prepared fluorescent photochromic diarylethenes having a bis-(phenylethynyl)anthracene or a perylenebisimide (PBI) unit.<sup>3–5</sup> Similar molecules have also been prepared by Hell et al.<sup>12,13</sup> In these molecules, the fluorescence spectrum overlaps well with the absorption spectrum of the closed-ring isomer of the DE unit, while the absorption spectrum of the open-ring isomer locates shorter than the fluorescence spectrum. Therefore, fluorescence quenching does not take place in the open-ring isomer, while the fluorescence is efficiently quenched by intramolecular energy transfer when the DE unit converts from the open- to the closed-ring isomers. Although the molecules are successfully used to demonstrate photoswitching of fluorescence at the single-molecule level,<sup>3–5</sup> unfortunately the fluorescence quenching inherently induces the cyclization reaction of the DE unit. The excited energy of the fluorescent unit is intramolecularly transferred to the closed-ring isomer and induces the ring-opening reaction. This reaction leads to the destruction of information in optical memories. For application to write-many-read-many (WORM) devices, the fluorescence switching and readout processes should be decoupled and independently controllable.

Received: November 29, 2010

Published: March 10, 2011

Scheme 1. Molecular Structures of Dyad 1, Model DE 2, and Model PBI 3



To overcome the problem of destructible readout, several methods or ideas have been proposed, such as readout using the changes of the refractive index or IR absorption at the wavelengths out of the switching unit,<sup>36–38</sup> stabilized signals by means of acid or base reactions,<sup>39</sup> switching of the electron-transfer efficiencies,<sup>40</sup> the molecular polarity,<sup>18</sup> or the supramolecular conformational changes,<sup>41</sup> and so on.<sup>42</sup> Although some of them have the potential to achieve non-destructive readout<sup>43</sup> in solid ensemble systems, no suitable molecular systems that can be applied at the single-molecule level have been developed due to inherent limitations of sensitivity, stability, and efficiency in their molecular properties and/or difficulty of operation in the solid state.

To avoid such problems and achieve reversible and efficient fluorescence photoswitching with non-destructive readout capability, we employed photoinduced electron transfer as the photoswitching mechanism.<sup>8,40</sup> The mechanism requires changing the oxidation/reduction potentials of the photoswitching DE unit. When the oxidation or reduction potential differences are large enough to induce electron transfer between the fluorescent unit and one of the isomers of the DE unit, isomerization of the DE unit induces the photoswitching of the fluorescence. The electron-transfer mechanism allows molecular design in such a manner that the absorption bands of both DE isomers are shorter than the

fluorescence spectrum of the fluorescent unit. The shorter absorption bands decouple the photochromic reaction from the fluorescence detection.

According to this concept, DE derivatives linked with fluorescent PBI have been synthesized.<sup>9–11</sup> Although the cycloreversion reaction along with the energy-transfer quenching was successfully avoided and efficient reversible fluorescence quenching via an electron transfer was observed, we failed to demonstrate non-destructive readout performance because of an unexpected photocyclization through the triplet state.<sup>11</sup> To prohibit the triplet route, we shifted the absorption spectrum of the PBI unit to longer wavelengths. When the  $S_1$  state of the PBI unit is lower than the  $T_1$  state of the DE unit, the triplet route is anticipated to be lost. After several trials, we succeeded in designing a diarylethene–perylenebisimide (DE-PBI) dyad (**1**, Scheme 1), which has non-destructive readout capability. Here we report on the fluorescence photoswitching and non-destructive fluorescence readout of **1** in solution as well as at a single-molecule level.

## RESULTS AND DISCUSSION

**Molecular Design.** Figure 1 shows the absorption and fluorescence spectra of component molecules [open- (**2a**) and

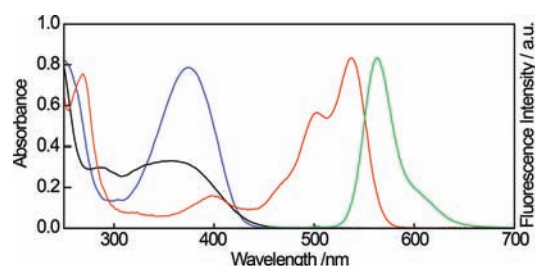


**Figure 1.** Absorption and fluorescence spectra of each component in 1,4-dioxane. Absorption spectra of the open-ring isomer of diarylethene unit (black), the closed-ring isomer of diarylethene unit (blue), and the PBI unit (red), and fluorescence spectrum of the PBI unit (green).

**Table 1. Reduction and Oxidation Potentials of Model DE 2 and PBI 3, Spectroscopic Excited-State Energy  $E_{00}$ , Center-to-Center Distances  $R_{cc}$  between DE Moiety and PBI Moiety, and Estimated Gibbs Free Energies  $\Delta G^\circ$**

compd	$E_{00}$ [eV]	$E_{red}$ ( $2^-/2$ ) [V] <sup>a</sup>	$E_{ox}$ ( $3^+/3$ ) [V] <sup>b</sup>	$R_{cc}$ [Å] <sup>c</sup>	$\Delta G^\circ$ [kcal/mol]
1a	2.25	-1.39	1.04	12.1	1.23
1b	2.25	-0.97	1.04	12.8	-8.55

<sup>a</sup> See ref 10. <sup>b</sup> See SI. <sup>c</sup> Center-to-center distances  $R_{cc}$  of both isomers were estimated from the AM1 calculation in MOPAC.

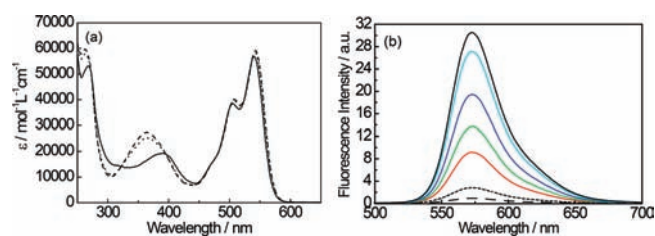


**Figure 2.** Absorption and fluorescence spectral changes of **1** in a binary solution (1,4-dioxane–methanol 50/50) upon irradiation with 445 and 365 nm light: open-ring isomer (**1a**) (solid line), the closed-ring isomer (**1b**) (dashed line), and the photostationary state under irradiation with 445 nm light (dotted line).

closed-ring isomers (**2b**) of the photochromic DE unit and fluorescent *N,N'*-bis(ethylpropyl)-1,7-bis[4-(1,1,3,3-tetramethylbutyl)phenoxy]perylene-3,4:9,10-tetracarboxylbisimide (**3**), Scheme 1] in 1,4-dioxane. The fluorescence spectrum of **3** does not overlap with the absorption spectra of **2a** and **2b**. Therefore, singlet–singlet intramolecular energy transfer from **3** to **2a** and **2b** is avoided. The absorption maximum of the PBI unit was observed at 537 nm, which is 15 nm longer than the maximum of PBI without 4-(tetramethylbutyl)phenoxy substituents.<sup>11</sup> The small red-shift prohibits the triplet route.

In order to explore the feasibility of an intramolecular electron-transfer photoswitching, energy gaps ( $\Delta G^\circ$ ) for charge separation in the excited states of **1a** and **1b** in a given solvent were estimated by applying the reduction and oxidation potentials of model compounds **2** and **3** to the Rehm–Weller equation (detailed parameters are shown in Table 1) (see Supporting Information (SI)).<sup>28</sup> The energy gaps ( $\Delta G^\circ$ ) were calculated to be 1.23 kcal/mol for the open-ring isomer (**1a**) and -8.55 kcal/mol for the closed-ring isomer (**1b**) in dichloromethane ( $\epsilon = 8.93$ ). From the energy values it is probable that electron transfer takes place only for the closed-ring isomer (**1b**) in dichloromethane.

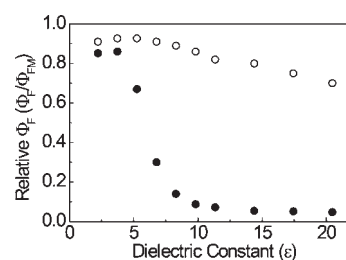


**Figure 3.** Relative fluorescence quantum yields as a function of dielectric constant for **1a** (○) and **1b** (●).

Dyad **1** was synthesized by procedures similar to those reported in a previous paper.<sup>10,44–46</sup> Detailed procedures of the synthesis and compound data are described in the SI.

**Fluorescence Photoswitching in Solution.** Figure 2a,b shows the absorption and fluorescence spectral changes upon irradiation with visible ( $\lambda = 445$  nm) and UV (365 nm) light in a binary solution (1,4-dioxane–methanol 50/50) ( $\epsilon = 17.4$ ) of **1**, respectively. Upon visible ( $\lambda = 445$  nm) light irradiation, the absorption band around 360 nm gradually increases. From the absorption spectrum of **1b** isolated by HPLC, the conversion from **1a** to **1b** in the photostationary state upon irradiation with 445 nm light was estimated to be 85%. Upon irradiation with UV (365 nm) light, the absorption spectrum turns back to the initial one (92%). Reversible fluorescence intensity change was also observed along with the photochromic reaction. When the solution reaches the photostationary state under irradiation with 445 nm light, the fluorescence intensity decreases to 14% of the initial value. The fluorescence intensity recovers upon UV (365 nm) light irradiation. On the other hand, in pure 1,4-dioxane ( $\epsilon = 2.21$ ), no fluorescence photoswitching was observed along with the photocyclization and photocycloreversion reactions of the DE unit (see SI Figure S2). This solvent dependence strongly suggests that the fluorescence quenching is caused by intramolecular electron transfer.

In order to closely elucidate the quenching mechanism, the relative fluorescence quantum yields of both isomers **1a** and **1b** were measured as a function of the dielectric constants of the solvents. Figure 3 shows the plots of the relative fluorescence quantum yields ( $\Phi_F/\Phi_{FM}$ ) of the isomer against the dielectric constants ( $\epsilon$ ) at room temperature (SI Table S1 summarizes the results). Binary mixtures of 1,4-dioxane and methanol were used to change the solvent dielectric constant. As can be seen from Figure 3,  $\Phi_F/\Phi_{FM}$  of **1a** decreases slightly with increasing dielectric constant. In contrast,  $\Phi_F/\Phi_{FM}$  of **1b** decreases dramatically when the dielectric constant increases above 5. In a binary polar solution (1,4-dioxane–methanol 40/60,  $\epsilon = 20.46$ ), the fluorescence is strongly quenched to  $\Phi_F/\Phi_{FM} < 0.047$ , while **1b** in pure 1,4-dioxane shows fluorescence intensity comparable to that of **1a**. No remarkable change in the absorption and fluorescence spectra depending on the solvent polarity was observed (see SI Table S2).

**Fluorescence Quenching Dynamics.** To directly elucidate the fluorescence quenching mechanism, time-resolved fluorescence and transient absorption spectral measurements were carried out. Figure 4a,b shows fluorescence decays of **1a** in pure 1,4-dioxane and in a 1,4-dioxane–methanol (50/50) binary solution, respectively. Both decays are well reproduced by single-exponential decay functions with time constants of  $4.9 \pm 0.1$  ns in 1,4-dioxane and  $3.9 \pm 0.1$  ns in the binary solution. These time constants are similar to those for **3** in both solutions (see SI),

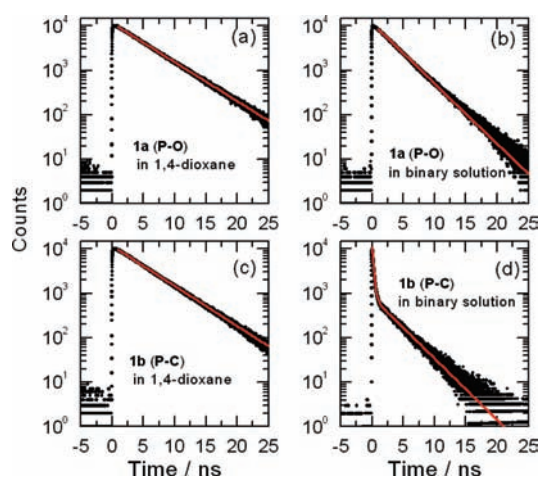


**Figure 4.** Fluorescence decays of **1a** and **1b** in pure 1,4-dioxane (a,c) and in a 1,4-dioxane–methanol (50/50) binary solution (b,d). Excitation and monitoring wavelengths were 532 and 570 nm, respectively. Instrumental response function (IRF) was 32 ps. Red lines are results calculated for the analysis (see text).

indicating that no effective quenching takes place in the excited PBI unit by the open-ring isomer in either solution. Figure 4c,d shows the fluorescence decays of **1b** in pure 1,4-dioxane and in the binary solution, respectively. The decay of **1b** in pure 1,4-dioxane is reproduced by single-exponential decay with a time constant of  $4.8 \pm 0.1$  ns. This time constant is similar to the fluorescence lifetime of **3** and **1a** in 1,4-dioxane, showing that no effective quenching of the PBI unit by the closed-ring isomer occurs in pure 1,4-dioxane. On the other hand, the decay in the binary solution shows rapid decay in the sub-nanosecond time region, followed by a further decay with a much longer time constant. The red line in Figure 4d is the curve calculated with a double-exponential decay function with the faster time constant of 200 ps and the slower one of 3.9 ns. Pre-exponential factors for the faster and the slower time constants are respectively 0.93 and 0.07. The fast decay of  $200 \pm 10$  ps indicates that the PBI unit in the fluorescent state is effectively quenched by the closed-ring isomer of the DE unit in the binary solution. On the other hand, the slower one might be due to the residual trace of **1a** in the solution.

To clarify the mechanism of the quenching directly, we employed transient absorption spectroscopy with a femtosecond laser pulse at 530 nm as an excitation source. Time evolution of transient absorption spectra of **1b** in 1,4-dioxane was ascribed to the deactivation of the  $S_1$  state of the PBI unit with a time constant of ca. 5 ns, which is in agreement with the fluorescence lifetime in 1,4-dioxane (see SI). This result indicates again that the  $S_1$  state of the PBI unit is not affected by the closed-ring isomer of the DE unit in pure 1,4-dioxane. On the other hand, time evolution of transient absorption spectra of **1b** in the binary solution (1,4-dioxane–methanol 50/50) showed rapid decay in a few hundreds of picoseconds time region (SI). The main time constants of the time profiles were 30 and 180 ps, the latter of which is in agreement with the fluorescence decay time constant of **1b** in the binary solution, as shown in Figure 4. The spectra corresponding to these two time constants, which were obtained by the analysis of time profiles with different monitoring wavelengths (SI), are exhibited in Figure 5. The component corresponding to the decay with 180 ps time constant is safely

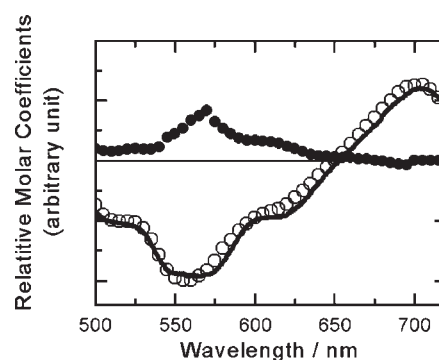


**Figure 5.** Spectra corresponding to 180 (○) and 30 ps (●) time constants, obtained by analysis of the time profiles of transient absorption of **1b** in a 1,4-dioxane–methanol (50/50) binary solution, excited with a femtosecond 530 nm laser pulse. The bold solid line is the  $S_n \leftarrow S_1$  absorption spectrum of PBI unit, measured for **1b** in pure 1,4-dioxane.

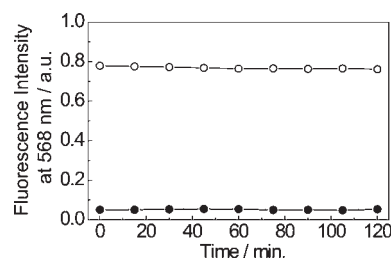


**Figure 6.** Non-destructive fluorescence readout capability of both open- and closed-ring isomers. Fluorescence intensities at 568 nm upon excitation at 532 nm of **1a** (○) and **1b** (●) were plotted against irradiation time. Both isomers had the same absorbance at 532 nm ( $\sim 0.1$ ).  $\lambda_{\text{ex}} = 532$  nm laser light ( $2.5 \text{ mW/cm}^2$ ).

attributed to the  $S_1$  state of the PBI unit on the basis of the spectral band shape and the absorption maxima.<sup>10</sup> On the other hand, the spectrum appearing with 180 ps and decaying with 30 ps time constants corresponds to the radical cation of PBI.<sup>10</sup> These results clearly lead to the conclusion that the charge separation reaction between the excited PBI unit and the closed-ring isomer of DE takes place with a time constant of 180 ps, followed by charge recombination with a 30 ps time constant.

**Non-destructive Fluorescence Readout.** Non-destructive fluorescence readout capability is an indispensable property for optical memories.<sup>8,18,36–42</sup> As mentioned in the Introduction, previous DE derivatives connected with the fluorescence unit lack the non-destructive fluorescence readout capability owing to the quenching by energy transfer<sup>3–5</sup> and contribution of the triplet channel in the photocyclization reaction.<sup>10,11</sup> On the other hand, the present dyad **1** gives the non-destructive performance. The small red-shift of the absorption spectrum of the PBI unit avoids the triplet channel. The fluorescence intensities at 568 nm of **1a** and **1b** stay constant even when the binary solution (1,4-dioxane–methanol 50/50) of **1a** and **1b** is irradiated with 532 nm laser light ( $2.5 \text{ mW/cm}^2$ ) for 2 h, as shown in Figure 6. Absorption spectral changes of both isomers were not observed even after 2 h. This result indicates that the absorbed energy of the PBI unit does not induce the isomerization of the DE unit. Non-destructive readout capability is achieved in this dyad system.

**Fluorescence Photoswitching at the Single-Molecule Level.** Fluorescence photoswitching and non-destructive readout were also observed at the single-molecule level. Samples were

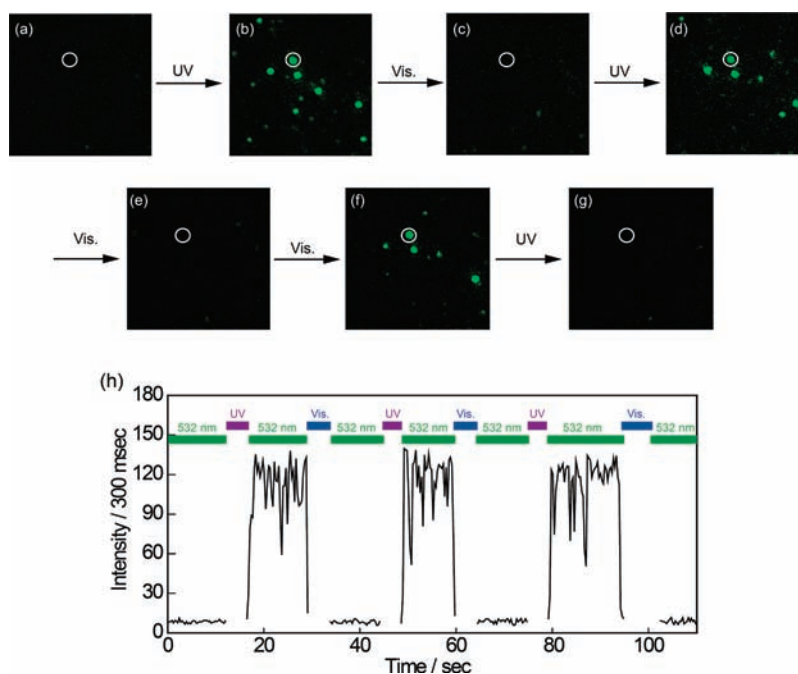


**Figure 7.** Single-molecule fluorescence photoswitching in a PMA thin film. (a–g) Wide-field fluorescence images of **1** embedded in a PMA thin film. Conditions: excitation wavelength, 532 nm from a solid laser; UV (330–380 nm) light; visible (440–490 nm) light; N<sub>2</sub> atmosphere; exposure time, 300 ms. (h) Time trace of fluorescence intensity of a single molecule of **1**, represented as a white circle in panels a–g. Green, violet, and blue bars indicate irradiation period with 532 nm laser light, UV light, and visible light, respectively.

prepared by spin-casting a toluene solution of 2 wt % poly-(methyl acrylate) (PMA,  $T_g = 9\text{ }^\circ\text{C}$ ) or 1.2 wt % Zeonex ( $T_g \approx 130\text{ }^\circ\text{C}$ ) containing **1b** ( $1.5 \times 10^{-11}\text{ M}$ ) to prepare all molecules in the photoreactive anti-parallel conformation. When closed-ring isomers are converted to the open-ring isomers, all molecules are in the anti-parallel conformation.<sup>1,4</sup> PMA, a polar and soft polymer, was selected as the host matrix in this study to observe the reversible photoswitching, referring to the recent result reported by Würthner and Brouwer's group.<sup>47</sup> Zeonex, an apolar and rigid polymer, was used to determine the environmental polarity dependence of the fluorescence photoswitching behavior.

Figure 7a–g shows the wide-field fluorescence microscopy images taken on the same area under irradiation with 532 nm as the fluorescence excitation light source (SI Movie S1). Visible (440–490 nm) light from a Hg lamp was used as the light source to induce the photocyclization reaction, and UV (330–380 nm) light from a Hg lamp was used as the light source to induce the photocycloreversion reaction. Initially, the PMA film containing **1b** shows a dark image under irradiation with only 532 nm laser light (Figure 7a). At 16.8 s, when UV light is irradiated to the sample for ca. 5 s, fluorescence bright spots corresponding to individual **1a** molecules appear (Figure 7b). After UV light irradiation is stopped, the fluorescent state persists under irradiation with 532 nm laser light. At 29.1 s, when visible light is irradiated onto the sample, the fluorescence bright spots disappear abruptly (Figure 7c). After stopping the visible light irradiation, the dark state remains until the next irradiation with UV light. These ON–OFF fluorescence switching behaviors can be observed several times (Figure 7d–g).

On the other hand, in the rigid apolar Zeonex polymer film containing **1**, no clear fluorescence switching was observed upon irradiation with visible and UV light (SI Figure S7). The fluorescence intensity of an individual molecule embedded in the Zeonex polymer film is constant upon visible and/or UV light irradiation.

Only one-step irreversible photobleaching was observed, as shown in SI Figure S7 (see also SI Movie S2). Intramolecular electron-transfer quenching of fluorescence requires polar environments. As evidenced in solution experiments, the fluorescence switching takes place only in polar environments.

Figure 7h shows the fluorescence intensity trajectory of one molecule, which is indicated by the white circle in Figure 7a–g. As can be seen in Figure 7h, one-step ON–OFF fluorescence switching is clearly observed upon visible and UV light irradiation. The fluorescence “OFF” state is initially observed under irradiation with only 532 nm laser light. The fluorescence “OFF” state changes to the fluorescence “ON” state in one step upon UV light irradiation. After stopping UV light irradiation, the fluorescence “ON” state remains stable during irradiation with only 532 nm laser light. The fluorescence “ON” state turns back to the fluorescence “OFF” state when visible light is irradiated onto the sample. After stopping visible light irradiation, the dark state remains until the next irradiation with UV light. The fluorescence switching is safely ascribed to the photochromic reaction of individual dyad **1**. It is worth noting that both fluorescence “ON” and “OFF” states remain stable during excitation with 532 nm laser light. The result clearly indicates that non-destructive fluorescence readout can be achieved even at the single-molecule level.

## CONCLUSION

A photoswitchable fluorescent DE-PBI dyad **1** was synthesized, and its fluorescence photoswitching and non-destructive fluorescence readout were studied in solution and at the single-molecule level. The fluorescence quantum yield of **1b** is strongly dependent on solvent polarity and decreases with increasing solvent dielectric constant. It is concluded from the time-resolved fluorescent and transient absorption spectroscopies that

the fluorescence is quenched by the intramolecular electron-transfer process. Non-destructive fluorescence readout upon excitation with 532 nm laser light is confirmed for both **1a** and **1b** under excitation with 532 nm laser light in solution as well as at the single-molecule level. The results indicate that the dyad system is useful for ultra-high-density optical memories and super-high-resolution fluorescence imaging.

## EXPERIMENTAL SECTION

**General.** General chemicals were purchased from Tokyo Chemical Industries, Wako Pure Chemicals, or Aldrich Chemical Co. and used without further purification. Solvents used in photochemical measurements were of spectroscopic grade and were purified by distillation before use.  $^1\text{H}$  NMR spectra were recorded on an NMR spectrometer (Bruker AVANCE 400, 400 MHz). Samples were dissolved in  $\text{CDCl}_3$  with tetramethylsilane as an internal standard. Mass spectra were measured with a mass spectrometer (Shimadzu GCMS-QP5050A and Applied Biosystems, Voyager). Cyclic voltammograms was measured by using an ALS-600 electrochemical analyzer. Absorption and fluorescence spectra were measured with a Hitachi U-3500 absorption spectrophotometer and a Hitachi F-2500 fluorescence spectrophotometer, respectively. Fluorescence quantum yields were determined by using monochromatic 500 nm as the excitation light source, a very dilute solution, the absorbance of which is less than 0.02 at the excitation wavelength for all solvents, and  $N,N'$ -bis(1-hexylheptyl)perylene-3,4,9,10-tetracarboxylbisimide ( $\Phi_f = 0.99$ , in dichloromethane) as the reference. Photoirradiation was carried out using an USHIO 500 W xenon lamp as the light sources. Monochromic light was obtained by passing the light through a monochromator (Jobin-Yvon) or a band-pass filter ( $\Delta\lambda_{1/2} = 15$  nm).

**Transient Absorption Measurements.** For the detection of dynamic behaviors in the femtosecond to nanosecond time region, a dual NOPA/OPA laser system was used for transient absorption measurements. The details of the system were described elsewhere.<sup>48,49</sup> Briefly, the output of a femtosecond Ti:sapphire laser (Tsunami, Spectra-Physics) pumped by the second harmonic generation of a continuous-wave  $\text{Nd}^{3+}:\text{YVO}_4$  laser (Millennia Pro, Spectra-Physics) was regeneratively amplified with 1 kHz repetition rate (Spitfire, Spectra-Physics). The amplified pulse (802 nm, 0.9 mJ/pulse energy, 85 fs fwhm, 1 kHz) was divided into two pulses with the same energy (50%). One of these pulses was guided into a non-collinear optical parametric amplifier (NOPA) system (TOPAS-white, Light-Conversion). The NOPA output can cover the wavelength region between 500 and 1000 nm, with 1–40 mW output energy and ca. 20 fs fwhm. In the present work, the excitation wavelength was set to 532 nm. The white light continuum, which was generated by focusing the fundamental light at 802 nm into a 1 mm  $\text{CaF}_2$  window, covers the wavelength region from 350 to 720 nm. Polarization of two pulses was set at the magic angle for the entire measurement. The signal and the reference pulses were respectively detected with multichannel photodiode array systems (PMA-10, Hamamatsu), and the detected signals were sent to a personal computer for further analysis. In order to correct the transient absorption spectrum for the dispersion of the probe light, we measured the optical Kerr effect of  $\text{CCl}_4$  and determined the wavelength-dependent arrival times of the femtosecond white light at the sample position. From the cross-correlation trace between the NOPA output and the super-continuum at the sample position, the response pulse duration was ca. 80 fs. A rotating sample cell with an optical length of 2 mm was used, and the absorbance of the sample at the excitation wavelength was set to  $\sim 1.0$ .

**Fluorescence Lifetime Measurements.** For the measurement of the fluorescence time profiles, the time-correlated single-photon counting (TCSPC) method using a picosecond  $\text{Nd}^{3+}:\text{YAG}$  laser (DPM-1000&SBR-5080-FAP, Coherent, 532 nm, fwhm ca. 30 ps) with

8 MHz repetition rate was employed. A photomultiplier tube (Hamamatsu Photonics, R3809U-50) with an amplifier (Hamamatsu Photonics C5594) and a counting board (PicoQuanta, PicoHarp 300) were used for signal detection. A monochromator was placed in front of the photomultiplier tube. The instrumental response function was estimated by the fwhm of the scattered light from a colloidal solution for the excitation light pulse. In the present measurements, it was 32 ps. For the evaluation of the analyzed result, we used a reduced  $\chi^2$  value.<sup>50,51</sup>

**Single-Molecule Fluorescence Detection.** For single-molecule measurements, molecules were sparsely distributed around 100 nm thin films of Zeonex and poly(methyl acrylate) (PMA) on clean quartz glass coverslips by spin-coating one drop of mixed solution of a  $\sim 10^{-11}$  M the closed-ring isomer (**1b**) and 1.2 wt % Zeonex or 2 wt % PMA in toluene at 4000 rpm. Single-molecule fluorescence imaging and fluorescence intensity trajectory collection were performed under a nitrogen atmosphere, using an inverted fluorescence optical microscope (Nikon, TEi) equipped with a  $100\times$  1.45 NA oil-immersion objective (Nikon), appropriate filters (Chroma and Semrock) to remove the excitation light, and a back-illuminated electron-cooled CCD camera (iXon, Andowr). Circularly polarized 532 nm light from a solid laser (Spectra Physics, Excelsior 532) was used as the excitation light source.

## ASSOCIATED CONTENT

**S Supporting Information.** Synthetic procedures, characterization data, electrochemical data, dielectric constant dependence of photophysical properties, photochromic property in a 1,4-dioxane solution, time-resolved spectroscopic data, control experiment of the single-molecule fluorescence switching, and two movie files concerning the single-molecule fluorescence detection in a PMA film and in a Zeonex film. This material is available free of charge via the Internet at <http://pubs.acs.org>.

## AUTHOR INFORMATION

### Corresponding Author

tuyoshi@es.hokudai.ac.jp; iriemi@rikkyo.ac.jp

## ACKNOWLEDGMENT

This work was partly supported by Grant-in-Aids for Scientific Research on Priority Areas “New Frontiers in Photochromism (471)” (No. 19050008) from the Ministry of Education, Culture, Sports, Science, and Technology (MEXT) of Japanese Government. T.F. acknowledges support from PREST, JST, and Grant-in-Aids for Young Scientist (B) (No. 21750149).

## REFERENCES

- (1) Irie, M. *Chem. Rev.* **2000**, *100*, 1685.
- (2) Giordano, L.; Jovin, T. M.; Irie, M.; Jares-Erijman, E. A. *J. Am. Chem. Soc.* **2002**, *124*, 7481–7489.
- (3) Irie, M.; Fukaminato, T.; Sasaki, T.; Tamai, N.; Kawai, T. *Nature* **2002**, *420*, 759.
- (4) Fukaminato, T.; Sasaki, T.; Tamai, N.; Kawai, T.; Irie, M. *J. Am. Chem. Soc.* **2004**, *126*, 14843.
- (5) Fukaminato, T.; Umemoto, T.; Iwata, Y.; Yokojima, S.; Yoneyama, M.; Nakamura, S.; Irie, M. *J. Am. Chem. Soc.* **2007**, *129*, 5932.
- (6) Tian, H.; Wang, S. *Chem. Commun.* **2007**, 781.
- (7) Yun, C.; You, J.; Kim, J.; Huh, J.; Kim, E. J. *Photochem. Photobiol. C: Photochem. Rev.* **2009**, *10*, 111.
- (8) Berberich, M.; Krause, A. M.; Orlandi, M.; Scandola, F.; Würthner, F. *Angew. Chem., Int. Ed.* **2008**, *47*, 6616.
- (9) Odo, Y.; Fukaminato, T.; Irie, M. *Chem. Lett.* **2007**, *36*, 240.

- (10) Fukaminato, T.; Tanaka, M.; Doi, T.; Tamaoki, N.; Katayama, T.; Mallick, A.; Ishibashi, Y.; Miyasaka, H.; Irie, M. *Photochem. Photobiol. Sci.* **2010**, *9*, 181.
- (11) Fukaminato, T.; Doi, T.; Tanaka, M.; Irie, M. *J. Phys. Chem. C* **2009**, *113*, 11623.
- (12) Bossi, M.; Belov, V.; Polyakova, S.; Hell, S. W. *Angew. Chem., Int. Ed.* **2006**, *45*, 7462.
- (13) Fölling, J.; Polyakova, S.; Belov, V.; van Blaaderen, A.; Bossi, M. L.; Hell, S. W. *Small* **2008**, *4*, 134.
- (14) Hu, D.; Tian, Z.; Wu, W.; Wan, W.; Li, A. D. Q. *J. Am. Chem. Soc.* **2008**, *130*, 15279.
- (15) Soh, N.; Yoshida, K.; Nakajima, H.; Nakano, K.; Imato, T.; Fukaminato, T.; Irie, M. *Chem. Commun.* **2007**, 5206.
- (16) Zhu, L.; Wu, W.; Zhu, M.-Q.; Han, J. J.; Hurst, J. K.; Li, A. D. Q. *J. Am. Chem. Soc.* **2007**, *129*, 3524.
- (17) Zou, Y.; Yi, T.; Xiao, S.; Li, F.; Li, C.; Gao, X.; Wu, J.; Yu, M.; Huang, C. *J. Am. Chem. Soc.* **2008**, *130*, 15750.
- (18) Liang, Y. C.; Dvornikov, A. S.; Rentzepis, P. M. *Proc. Natl. Acad. Sci. U.S.A.* **2003**, *100*, 8109.
- (19) Tsien, R. Y. *Annu. Rev. Biochem.* **1998**, *67*, 509.
- (20) Ando, R.; Mizuno, H.; Miyawaki, A. *Science* **2004**, *306*, 1370.
- (21) Dickson, R. M.; Cubitt, A. B.; Tsien, R. Y.; Moerner, W. E. *Nature* **1997**, *388*, 355.
- (22) Moerner, W. E. *J. Phys. Chem. B* **2002**, *106*, 910.
- (23) Habuchi, S.; Ando, R.; Dedecker, P.; Verheijen, W.; Mizuno, H.; Miyawaki, A.; Hofkens, J. *Proc. Natl. Acad. Sci. U.S.A.* **2005**, *102*, 9511.
- (24) Andresen, M.; Wahl, M. C.; Steal, A. C.; Grater, F.; Schafer, L. V.; Trowitzsch, S.; Weber, G.; Eggeling, C.; Grubmüller, H.; Hell, S. W.; Jakobs, S. *Proc. Natl. Acad. Sci. U.S.A.* **2005**, *102*, 13070.
- (25) Flors, C.; Hotta, J.-I.; Uji-i, H.; Dedecker, P.; Ando, R.; Mizuno, H.; Miyawaki, A.; Hofkens, J. *J. Am. Chem. Soc.* **2007**, *129*, 13970.
- (26) Dedecker, P.; Hotta, J.-I.; Flors, C.; Sliwa, M.; Uji-i, H.; Roelfaers, M. B. J.; Ando, R.; Mizuno, H.; Miyawaki, A.; Hofkens, J. *J. Am. Chem. Soc.* **2007**, *129*, 16132.
- (27) An overview of optical data storages based on photoswitchable fluorescent proteins: Adam, V.; Mizuno, H.; Grichine, A.; Hotta, J.-I.; Yamagata, Y.; Moeyaert, B.; Nienhaus, G. U.; Miyawaki, A.; Bourgeois, D.; Hofkens, J. *J. Biotechnol.* **2010**, *149*, 289.
- (28) Holman, M. W.; Liu, R.; Zang, L.; Yan, P.; DiBenedetto, S. A.; Bowers, R. D.; Adams, D. M. *J. Am. Chem. Soc.* **2004**, *126*, 16126.
- (29) Heilemann, M.; Margeat, E.; Kasper, R.; Sauer, M.; Tinnefeld, P. *J. Am. Chem. Soc.* **2005**, *127*, 3801.
- (30) Hell, S. W.; Wichmann, J. *Opt. Lett.* **1994**, *19*, 780.
- (31) Hell, S. W. *Nat. Biotechnol.* **2003**, *21*, 1347.
- (32) Betzig, E.; Patterson, G. H.; Sougrat, R.; Lindwasser, O. W.; Olenych, S.; Bonifacino, J. S.; Davidson, M. W.; Lippincott-Schwartz, J.; Hess, H. F. *Science* **2006**, *313*, 1642.
- (33) Hell, S. W. *Science* **2007**, *316*, 1153.
- (34) Heilmann, M.; van de Linde, S.; Schüttelpelz, M.; Kasper, R.; Seefeldt, B.; Mukherjee, A.; Tinnefeld, P.; Sauer, M. *Angew. Chem., Int. Ed.* **2008**, *47*, 6172.
- (35) Heilemann, M.; Dedecker, P.; Hofkens, J.; Sauer, M. *Laser Photon. Rev.* **2009**, *3*, 180.
- (36) Kardinahl, T.; Franke, H. *Appl. Phys. A: Mater. Sci. Process.* **1995**, *61*, 23.
- (37) Seibold, M.; Port, H. *Chem. Phys. Lett.* **1996**, *252*, 135.
- (38) Uchida, K.; Saito, M.; Murakami, A.; Kobayashi, T.; Nakamura, S.; Irie, M. *Chem.—Eur. J.* **2005**, *11*, 534.
- (39) Yokoyama, Y.; Yamane, T.; Kurita, Y. *J. Chem. Soc., Chem. Commun.* **1991**, 1722.
- (40) Myles, A. J.; Branda, N. R. *J. Am. Chem. Soc.* **2001**, *123*, 177.
- (41) Kärnbratt, J.; Hammarson, M.; Li, S.; Anderson, H. L.; Albinsson, B.; Andréasson, J. *Angew. Chem., Int. Ed.* **2010**, *49*, 1854.
- (42) Lim, S.-J.; Seo, J.; Park, S. Y. *J. Am. Chem. Soc.* **2006**, *128*, 14542.
- (43) “Non-destructive readout” means that readout light does not influence the written information.
- (44) Jeong, Y.-C.; Yang, S. I.; Ahn, K.-H.; Kim, E. *Chem. Commun.* **2005**, 2503.
- (45) Jeong, Y.-C.; Yang, S. I.; Kim, E.; Ahn, K.-H. *Tetrahedron* **2006**, *62*, 5855.
- (46) Fukaminato, T.; Tanaka, M.; Kuroki, L.; Irie, M. *Chem. Commun.* **2008**, 3924.
- (47) Siekierzycka, J. R.; Hippius, C.; Würthner, F.; Williams, R. M.; Brouwer, A. M. *J. Am. Chem. Soc.* **2010**, *132*, 1240.
- (48) Miyasaka, H.; Murakami, M.; Okada, T.; Nagata, Y.; Itaya, A.; Kobatake, S.; Irie, M. *Chem. Phys. Lett.* **2003**, *371*, 40.
- (49) Ishibashi, Y.; Murakami, M.; Miyasaka, H.; Kobatake, S.; Irie, M.; Yokoyama, Y. *J. Phys. Chem. C* **2007**, *111*, 2730.
- (50) O’Connor, D. V.; Phillips, D. *Time-Correlated Single-Photon Counting*; Academic Press: London, 1984.
- (51) Boens, N.; et al. *Anal. Chem.* **2007**, *79*, 2137.